Real-time, seconds-resolved measurements of plasma methotrexate in situ in the living body

Alejandro Chamorro-Garcia, Julian Gerson, Charlotte Flatebo, Lisa Fetter, Alex M. Downs, Nicole Emmons, Herbert L. Ennis, Nenad Milosavić, Kyungae Yang, Milan Stojanovic, Francesco Ricci, Tod E. Kippin, and Kevin W. Plaxco*

Corresponding author: Kevin W. Plaxco; kwp@ucsb.edu
KEYWORDS: Biosensors, methotrexate, aptamers, drug monitoring, electrochemical sensors.

ABSTRACT: Dose-limiting toxicity and significant patient-to-patient pharmacokinetic variability often render it difficult to achieve the safe and effective dosing of drugs. This is further compounded by the slow, cumbersome nature of the analytical methods used to monitor patient-specific pharmacokinetics, which inevitably rely on blood draws followed by post-facto laboratory analysis. Motivated by the pressing need for improved "therapeutic drug monitoring," we are developing electrochemical aptamer-based (EAB) sensors, a minimally invasive biosensor architecture that can provide real-time, seconds-resolved measurements of drug levels in situ in the living body. A key advantage of EAB sensors is that they are generalizable to the detection of a wide range of therapeutic agents because they are independent of the chemical or enzymatic reactivity of their targets. Three of the four therapeutic drug classes that have, to date, been shown measurable using in-vivo EAB sensors, however, bind to nucleic acids as part of their mode of action, leaving open questions regarding the extent to which the approach can be generalized to therapeutics that do not. Here we demonstrate real-time, in-vivo measurements of plasma methotrexate, an antimetabolite (a mode of action not reliant on DNA binding) chemotherapeutic, following human-relevant dosing in a live rat animal model. By providing hundreds of drug concentration values, the resulting seconds-resolved measurements succeed in defining key pharmacokinetic parameters, including the drug's elimination rate, peak plasma concentration, and exposure (area under the curve), with unprecedented, 5 to 10% precision. With this level of precision, we easily identify significant (>2-fold) differences in drug exposure occurring between even healthy rats given the same mass-adjusted methotrexate dose. By providing a real-time, seconds-resolved window into methotrexate pharmacokinetics, such measurements can be used to precisely "individualize" the dosing of this significantly toxic, yet vitally important chemotherapeutic.

Introduction

The minimum toxic dose of some drugs is close to their required therapeutic dose, rendering their therapeutic windows narrow. When patient-to-patient metabolic variability is small, this does not represent a significant problem. For example, although the ratio of an effective dose to a toxic dose (the so-called therapeutic ratio) is less than 5 for acetaminophen, the drug's pharmacokinetic variability is low enough that it is considered safe to provide "over the counter."[1] In contrast, however, the therapeutic ratios of some drugs are quite small relative to inter-patient pharmacokinetic variability, and thus care is required to achieve individualized dosing that is both effective and safe.[2,3] Indeed, for some drugs the day-to-day variability within individuals can be clinically significant,[4–7] with the greatest variability often being seen in grievously ill patients, the very population for whom the margin for clinical error is smallest.[4,5,7] The "therapeutic drug monitoring" required to safely and effectively deliver drugs with dangerously narrow therapeutic windows, however, currently requires blood draws and laboratory analysis, rendering it cumbersome and slow, and typically limiting it to a once-a-day "snapshot" view into a patient's drug levels.[8] With so few data points, the accuracy with which standard therapeutic drug monitoring defines individualized pharmacokinetics is poor, and its ability to detect health-status-driven, hour-to-hour changes in an individual patient's pharmacokinetics is effectively non-existent.

In response to the need to improve therapeutic drug monitoring we are developing electrochemical, aptamer-based (EAB) sensors (**Fig. 1A**), a technology that, in contrast to established monitoring approaches, provides real-time, seconds-resolved information on in-vivo drug levels.[9–12] By analogy to the impact continuous glucose monitors have had on the treatment of diabetes, EAB sensors could thus revolutionize the delivery of therapeutic drugs by enabling the achievement of accurate and consistent drug levels across patients.[13,14] To achieve such performance, EAB sensors are comprised of a redox-reporter-modified aptamer attached to a gold electrode via a self-assembled monolayer.[15,16] Upon target binding, the aptamer undergoes a conformational change, producing an easily-measurable shift in the electrochemical output of the reporter (Fig. 1B). Because this signal transduction mechanism is reagentless, wash- and incubation-free, and rapidly reversible, EAB sensors support high frequency, real-time molecular monitoring. And because it mimics the conformation-linked signaling seen in naturally occurring chemoperception systems, EAB sensors are selective enough to perform well in complex environments, even when placed inside the living

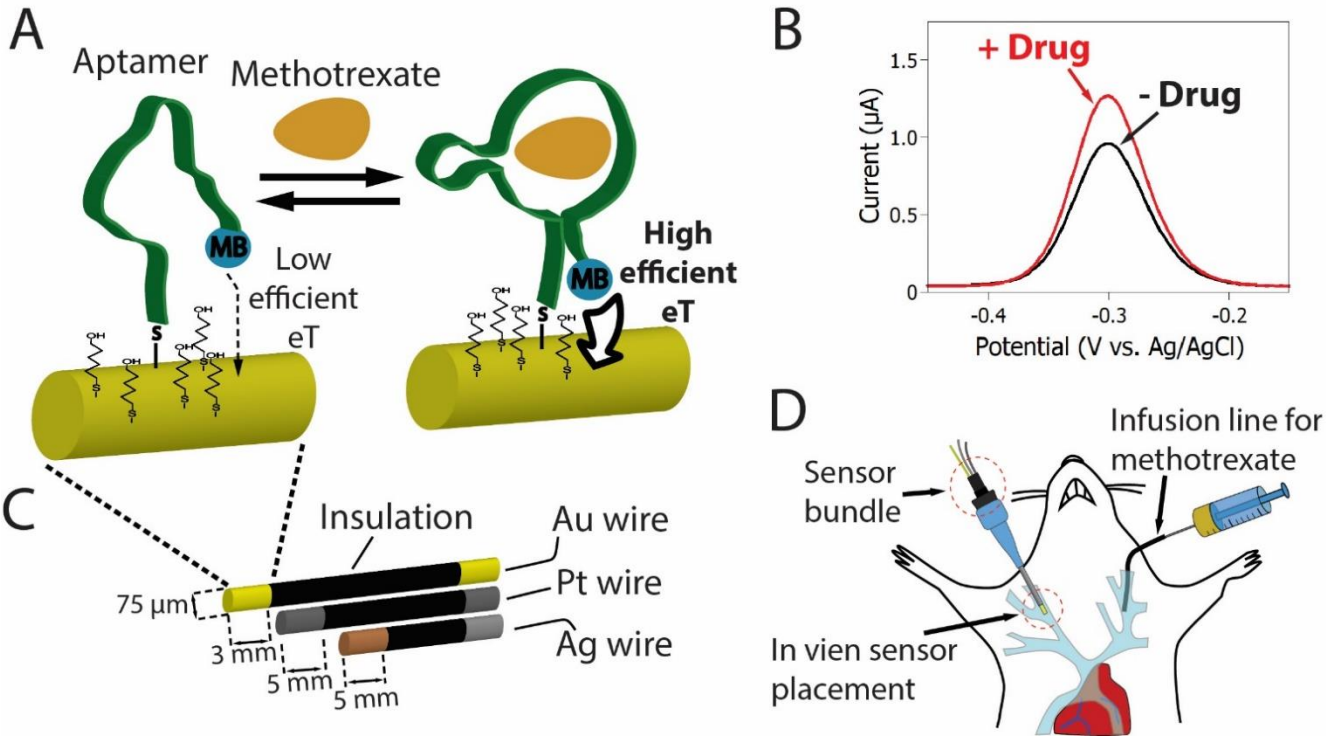

Figure 1. (**A**) Electrochemical aptamer-based (EAB) sensors are comprised of a target-binding aptamer attached via a thiol on one terminus to an interrogating electrode and modified, typically at the terminus distal to the electrode, with a redox reporter (here methylene blue: MB). Target binding induces a conformational change, altering in turn the rate of electron transfer from the attached redox reporter. (**B**) This leads to an easily detectable change in peak current when the sensor is interrogated using square wave voltammetry. (**C**) We fabricate EAB sensors using 75 μm diameter, 3 mm long gold working electrode, bundled with same-diameter, 5 mm long platinum counter and silver/silver-chloride reference electrodes. (**D**) The completed sensor is emplaced in the external jugular vein of a rat via a 22-gauge guide catheter and used to monitor in real time methotrexate levels.

body.[9–12,17,18] Indeed, using the real-time data provided by in-vivo EAB sensors we have demonstrated closed-loop, feedback-controlled drug delivery that achieves unprecedented precision and accuracy in the delivery of narrow-therapeutic-window antibiotics.[10,11]

Prior to EAB sensors, all in-vivo molecular measurement technologies had relied on the enzymatic degradation (e.g., glucose, lactate, glutamine, acetylcholine, and penicillin)[19–21] or intrinsic chemical reactivity (e.g., the covalent binding of oxygen to hemoglobin, the electrochemical oxidation of neurotransmitters)[20,22] of their targets, greatly limiting the extent to which in-vivo molecular monitoring could be expanded to new targets. EAB sensors, in contrast, rely on non-covalent binding, and not the specific chemical reactivity of the target. In theory, this renders the approach generalizable to the detection of a wide range of therapeutic drugs. In practice, however, the scope of the EAB platform remains to be determined. For example, while we have previously demonstrated the in-vivo monitoring of clinically-relevant concentrations of the aminoglycoside antibiotics,[9,23] the chemotherapeutics doxorubicin and irinotecan,[9,12] and the glycopeptide antibiotic vancomycin,[11] three of these four targets bind to nucleic acids as their mode of action. Specifically, the aminoglycosides kill bacteria by binding their ribosomal RNA, doxorubicin inhibits topoisomerase II by intercalating into double-stranded DNA, and irinotecan inactivates topoisomerase 1 by stacking against the base pairs flanking the topoisomerase-induced cleavage site. Given their "naturally high" affinities for nucleic acids, these drugs may be particularly amenable to detection using aptamers, leaving the true breadth of the EAB approach unresolved.

With the question of platform versatility in mind, here we have characterized the in-vivo performance of an EAB sensor against methotrexate, an antimetabolite chemotherapeutic[24] that does not bind to nucleic acids as part of its mode of action. Initially known as amethopterin, methotrexate remains in widespread therapeutic use 70 years after it was discovered and is included in the World Health organization's list of essential medicines. A folic acid analogue, methotrexate competitively inhibits the enzyme dihydrofolate reductase, preventing it from transforming dihydrofolate into tetrahydrofolate which inhibits de novo DNA synthesis and, with that, the growth of cancer cells.[25] When applied in cancer treatment, however, methotrexate suffers from dose-limiting toxicity, rendering therapeutic drug monitoring a key element of its associated standard of care.[26–30] Currently, mass spectrometry remains the gold standard for methotrexate monitoring,[31] time resolution of which is severely limited due to its reliance on blood draws (for sample collection). Likewise, its reliance on laboratory-based analysis leads to long lag times (i.e., hours or days), negating the ability to perform the matching of dose to patient drug levels within a treatment session. And while several other authors have described potentially more convenient sensors for the detection of methotrexate,[32–35] none have been shown to support real time in-vivo measurements. Thus, in addition to speaking to the versatility of our approach, the successful demonstration of a methotrexate-detecting, in-vivo EAB sensor could also pave the way for improved precision in the delivery of this important chemotherapeutic.

Results

For this work we adapted a previously described, in vitro sensor against methotrexate[36] for use in-vivo in our rat animal model. To do so we used thiol-on-gold self-assembled monolayer chemistry to attach the 3' end of a 40-base, methotrexate-binding aptamer to a 75 μm diameter, 3 mm long gold wire working electrode (**Fig. 1A**), as used in previous in-vivo studies[9,37].

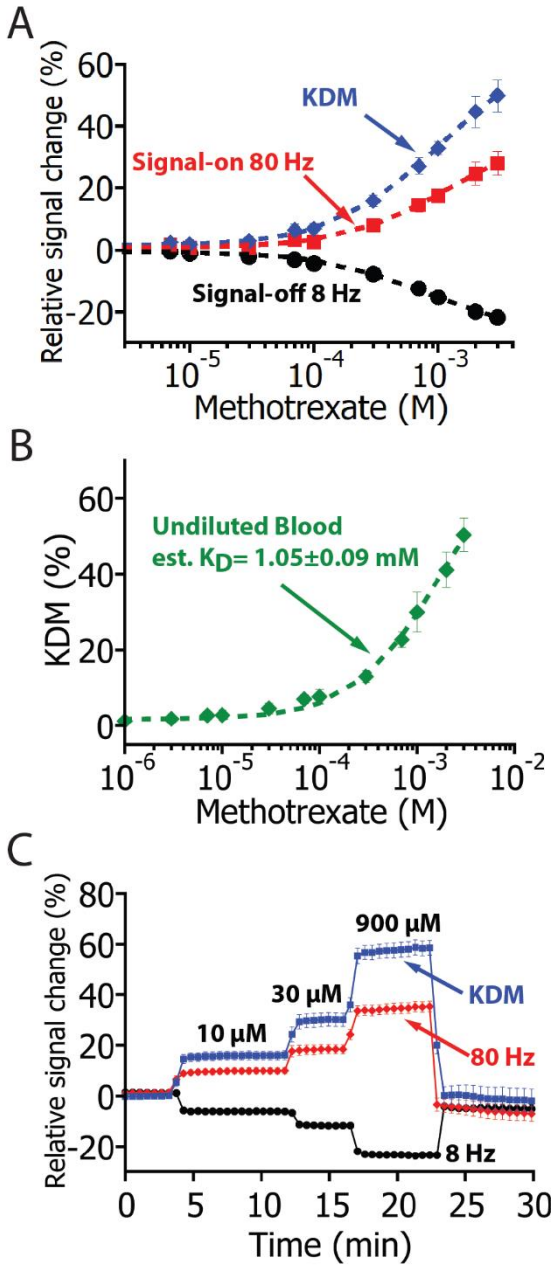

Figure 2. (**A**) Aptamer based electrochemical (EAB) sensors can be tuned to be signal-on (signaling current increases upon the addition of target) or signal-off by changing the square-wave frequency employed in their interrogation. Taking the difference between these two signals (kinetic differential measurements, KDM) increases gain and reduces drift.[9,38] The

data shown here were collected in vitro in undiluted whole blood at 37˚C. (**B**) The resulting binding curve of the EAB sensor when titrated at 37 °C matches the methotrexate levels seen in high-dose treatment, scenario in which therapeutic drug monitoring is of the greatest value.[26–28,39]. Not reaching sensor's saturation, the K_D we show is the estimated K_D value that we obtained and used for calculating methotrexate concentration (**C**) The EAB sensor responds rapidly and reversibly to its target. For example, when challenged with sequential additions of methotrexate the sensor responds within the time (here 30 s) it takes to perform the pair of square wave voltammetry scans needed to perform KDM. Note: the error bars shown in this figure reflect the standard deviation of replicate measurements made using independently fabricated sensors.

We then insulated this with polytetrafluoroethylene, bundled it with similar-dimension chloride-anodized silver wire reference and platinum wire counter electrodes, and placed the three into a 22-gauge catheter for later intravenous insertion.[40] When interrogated a square wave frequency of 80 Hz the signaling current of the resulting sensor increases upon target binding (**Fig. 2A**, red curve). In contrast, at a square wave frequency of 8 Hz the sensor's output falls in response to target (**Fig. 2A**, black curve). Taking the difference between these two signals (**Fig. 2A**, blue curve), an approach termed Kinetic Differential Measurements (KDM),[9,38,41] leads to improved gain (the relative change in signal seen between zero and saturating target).

The methotrexate-detecting EAB sensor achieves clinically relevant sensitivity and physiologically relevant time resolution in the measurement of its target. When challenged in whole blood at 37˚C, for example, the sensor's dissociation constant is 1.05±0.09 mM, leading to good overlap between the sensor's useful dynamic range and the few-hundred micromolar plasma concentrations seen in high dose methotrexate therapies.[26,42,43] The sensor's time resolution is likewise sufficient to perform high-precision monitoring of the drug's pharmacokinetics, the most rapid phase of which has a timescale of several minutes.[44] Specifically, rapid mixing experiments indicate that, following both clinically relevant increases and decreases in methotrexate concentrations, the sensor equilibrates within the time required to collect the paired voltammetric scans needed to perform KDM, rendering the latter time (22 s for our in-vivo measurements) the time resolution of the sensor (**Fig. 2C**).

The methotrexate-detecting EAB sensor provides a highly-time resolved, real-time approach to monitoring plasma methotrexate levels. To see this, we placed a sensor in situ in the jugular of a live rat and then challenged the animal with the drug at 300 mg/kg infused intravenously over 3 min. Doing so we observed a rapid rise in plasma levels to a peak concentration, C_{max}, of 600±40 μM (**Fig. 3**), a value falling well within the 500-1000 μM range seen in both high-dose human therapies[29,42,45] and rat models of such therapy.[44,46] Following the end of infusion the drug level subsequently falls with pharmacokinetics matching the known elimination rate of this drug in rats.[44] When we follow this first infusion with a second infusion of the same dose, we observe good pharmacokinetic reproducibility between the two drug exposures.

Prior researchers have used two and three compartment models[45,47,48] to fit the pharmacokinetics of methotrexate. The amplitudes of the second and third phase or phases, however are quite small and their timescales are quite long. Scheufler and co-workers[48], for example, reported a rapid phase (11 min lifetime) of amplitude 330 μM, and two additional, slower phases (of lifetimes 37.5 min and 6 h) whose combined amplitudes reach only 70 μM. That is, more than 80% of the total change in concentration is captured in the most rapid of the three phases, which is the phase that dominates our observation period. Given this, we fit our sequential injection data to a single-exponential model.[44] Doing so we find that the observed elimination time constants, which are 32.5±2.4 and 34.1±2.1 min for the first and second infusions, respectively, are within error between the two challenges (**Fig. 3**). Likewise, the two areas under the curve (AUC) are, at 325±38 and 396±42 μM·h respectively, are quite similar. In contrast, we see a small, but statistically significant difference in C_{max} between the two challenges, as these reach 600±40 and 730±40 μM, respectively. This difference presumably occurred because we began the second challenge before the animal had completely eliminated the drug delivered in the first challenge.

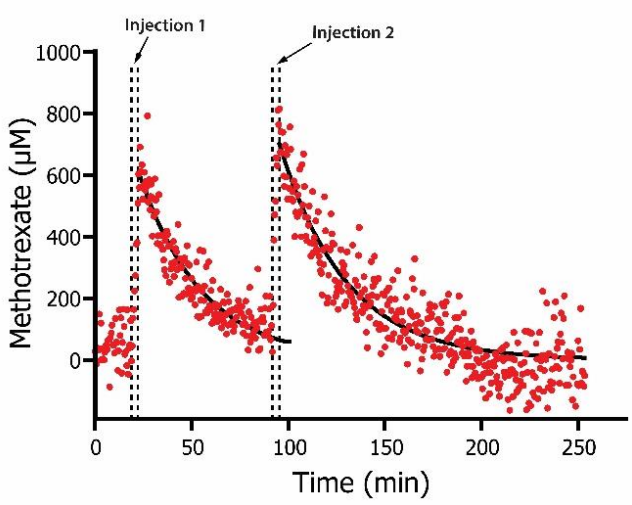

Figure 3. In-vivo EAB sensors provide a ready means of monitoring plasma methotrexate levels in real time. Dotted lines mark the point in time of beginning and end of infusion period. As shown here, for example, a KDM-corrected sensor placed in situ in the jugular of a live rat measures a rapid rise to plasma concentrations matching those seen after the end of infusion in high-dose human methotrexate treatment after a 300 mg/kg intravenous dose of methotrexate (rat weight: 680 g). Following the end of the infusion, plasma drug concentrations then return to baseline following first-order elimination kinetics.[41] A second, identical infusion illustrates the good pharmacokinetic reproducibility we observe. The solid black lines are fits to a one-compartment pharmacokinetic model. The peak plasma concentrations (Cmax = 600±40 and 730±50 μM respectively), elimination time constants (32.5±2.4 and 34.1±2.1 min), and AUCs (325±38 and 396±42 μM·h) were derived from these fits, with an R2 of 0.85 and 0.87 for the first and second injections respectively. The reported confidence intervals reflect the 95% confidence intervals calculated from the fits.

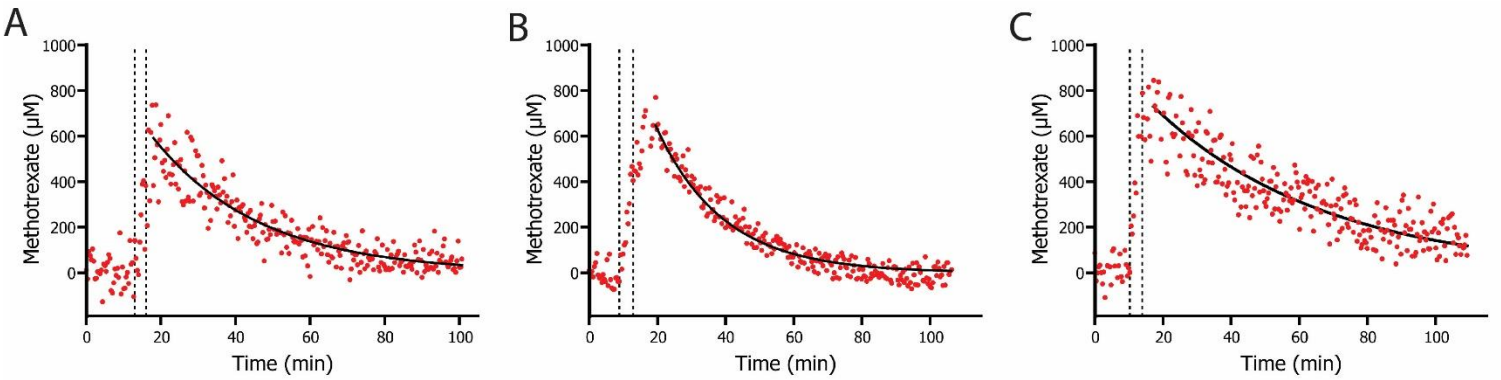

Figure 4. Highlighting the potential value of therapeutic drug monitoring, the pharmacokinetics of methotrexate exhibit significant inter-animal variability. Presented here, for example, are the responses of three individual rats (of weights 468, 488 and 460 grams) to 300 mg/kg intravenous dose. The solid black line is the fit to a one-compartment pharmacokinetic model. Achieving peak plasma concentrations of 595±78, 675±65 and 736±96 μM respectively, elimination time constants of 28.8±3.2, 19.7±1.0, and 50.5±3.4 min, and areas under the curve (AUC) of 268±36, 217±20 and 510±52 μM·h. (See Fig. SI2 for the raw data prior to KDM drift correction).

The relative convenience of EAB sensor measurements provides a ready opportunity to monitor pharmacokinetic variability between subjects. To see this, we next challenged three Sprague Dawley rats with the same mass-adjusted (300 mg/kg) intravenous dose (**Fig. 4**) and fitted the resulting pharmacokinetics to a one-compartment model. Doing so we found that the C_{max} observed for all three animals fall within error of one another, as perhaps expected for such mass-adjusted dosing, which easily accounts for differences in the animals' plasma volumes.[49] In contrast, the elimination lifetimes of the three animals varied significantly, ranging from 19.7±1.0 to 50.5±3.4 min. Because of this, the AUCs of the three animals also varied significantly, ranging from 217±20 to 510±52 μmol·h·L-1. That we see such highly variable drug exposure among healthy, similar size and age rats receiving the same mass-adjusted doses highlights the need for therapeutic drug monitoring in guiding individualized therapies.

The relative convenience of EAB sensor measurements provides a ready opportunity to monitor pharmacokinetic variability between subjects. To see this, we next challenged three Sprague Dawley rats with the same mass-adjusted (300 mg/kg) intravenous dose and fitted the resulting pharmacokinetics to a one-compartment model. Doing so we found that the C_{max} observed for all three animals fall within error of one another, as perhaps expected for such mass-adjusted dosing (**Fig. 4**), which easily accounts for differences in the animals' plasma volumes.[49] In contrast, the elimination lifetimes of the three animals varied significantly, ranging from 19.7±1.0 to 50.5±3.4 min. Because of this, the AUCs of the three animals also varied significantly, ranging from 217±20 to 510±52 μmol·h·L^{-1}. That we see such highly variable drug exposure among healthy, similar size and age rats receiving the same mass-adjusted doses highlights the need for therapeutic drug monitoring in guiding individualized therapies.

Discussion

Here we have demonstrated the seconds-resolved, real-time measurement of plasma methotrexate concentrations in situ in the veins of live rats after dosing equivalent to high-dose methotrexate treatment in humans. This successful demonstration expands the in-vivo EAB molecular monitoring platform to the measurement of the fifth therapeutic drug or drug class over all (after the aminoglycosides,[10,41] doxorubicin,[9,38] irinotecan,[12] and vancomycin[11]) and to a second drug (after vancomycin) lacking significant intrinsic affinity for nucleic acids. When coupled with prior examples of the in-vivo monitoring of metabolites[17,18] and drugs-of-abuse,[9,50] which also lack intrinsic affinity for nucleic acids, the generality of the EAB platform, which arises due to the approach's being independent of the chemical reactivity of its targets, is becoming increasingly well established.

The methotrexate pharmacokinetics we observe are consistent with the results of prior studies of similarly high-dose methotrexate treatment in rats, providing a valuable "quality check" on our EAB-derived in-vivo data. These prior studies, however, achieved far poorer time resolution (typically fewer than 12 measurements per hour) and were typically averaged over multiple animals. For example, a study by Bremnes and co-workers[44], which employed ex-vivo measurements of radiolabeled drug in serum, collected 8 data points in the first hour. Similarly, Ekstrøm and co-workers[51], who monitored methotrexate in rats using microdialysis from venous blood, and Liu and co-workers[52], who performed ex-vivo measurement (liquid chromatography-mass spectrometry) of plasma methotrexate, each collected only 5 points over the first 2 h of their experiments. In all three cases, the experiments then averaged their data over 6 to 12 animals to determine population-averaged pharmacokinetics, raising questions regarding the extent to which the observed multi-exponential behavior is due to the multicompartmental

pharmacokinetics of the drug or arises due to inter-animal variability. In contrast, using EAB sensors we have sampled 150 points per hour, allowing for high-precision estimation of the pharmacokinetics of individual animals.

The ability to monitor in-vivo methotrexate concentrations conveniently and in real time could be of significant medical value. Specifically, the treatment of many cancers,[26–28] including acute lymphoblastic leukemia, osteosarcoma, and lymphomas,[24,53] entails such high methotrexate doses that clinically-significant nephrotoxicity is seen in approximately one third of patients,[54] with 12% progressing on to acute kidney injury.[55] To minimize this risk, body surface area estimates are currently used in an attempt to correct for patient-specific differences in the drug's clearance rate and distribution volume. The accuracy of this as a pharmacokinetic predictor, however, is questionable,[56] and appears to be particularly problematic in some patient groups, such as the obese.[57] Further complicating methotrexate dosing, the drug is 80% renally cleared,[58,59] and thus reductions in kidney function arising due to disease or to methotrexate toxicity can further increase drug exposure. Given these mechanisms, using laboratory-based therapeutic monitoring to ensure that methotrexate exposure remains within the acceptable risk/benefit window and to identify when countermeasures should be employed[60] has already proven of significant clinical value,[26,27] despite its limited time resolution (typically one measurement per day).[28,31,61] Although human clinical trials will be required, obviously, in order to confirm this, we believe it a reasonable assumption that the high-resolution, real-time information EAB sensor could substantially improve on this current standard of care.

Beyond the use of EAB measurements as a means of performing more convenient, higher precision therapeutic drug monitoring, it is important to also consider the potential impact of the real-time nature of the information it provides. Specifically, the real-time concentration monitoring provided by EAB sensors can easily support the closed-loop, feedback-controlled delivery of methotrexate (or, even, the antidotes to methotrexate toxicity, such as leucovorin or glucarpidase)[60] and other drugs with dangerously narrow or otherwise complex optimal dosing regimens. For example, using the real-time plasma concentration information provided by in-vivo EAB sensors we have already demonstrated the ability to maintain the plasma drug levels constant to a precision of better than ±20% over many hours in our rat animal model.[11,41] Likewise, using EAB sensors we have similarly demonstrated the ability to track with high-precision pre-defined, time-varying plasma drug time courses.[41,62] In short, the adaptation of in-vivo EAB sensors could ensure that drugs characterized by dangerously narrow therapeutic windows or highly complex, time-varying optimal plasma time courses can be delivered safely and effectively to even the most grievously ill, most metabolically unstable patients.

ASSOCIATED CONTENT

"This material is available free of charge via the Internet at http://pubs.acs.org."

AUTHOR INFORMATION

Corresponding Author

*Kevin W. Plaxco; kwp@ucsb.edu

Authors

Alejandro Chamorro-Garcia *- Department of Chemistry and Biochemistry, University of California, Santa Barbara, Santa Barbara, California 93106, USA; Dipartimento di Scienze e Tecnologie Chimiche, University of Rome, Tor Vergata, Via della Ricerca Scientifica, 00133 Rome, Italy.*

Julian Gerson *- Department of Psychological and Brain Sciences, University of California, Santa Barbara, Santa Barbara, California 93106, USA.*

Charlotte Flatebo *– Institute for Collaborative Biotechnologies, University of California Santa Barbara, Santa Barbara, CA 93106, USA.*

Lisa Fetter *- Biomolecular Science and Engineering Program, University of California, Santa Barbara, Santa Barbara, California 93106, USA.*

Alex M. Downs *- Department of Mechanical Engineering, University of California, Santa Barbara, Santa Barbara, California 93106, USA. Institute for Collaborative Biotechnologies, University of California Santa Barbara, Santa Barbara, CA 93106, USA.*

Nicole Emmons *- Department of Psychological and Brain Sciences, University of California, Santa Barbara, Santa Barbara, California 93106, USA.*

Herbert L. Ennis *- Department of Medicine, Columbia University, New York, New York 10032, United States.*

Nenad Milosavic *- Department of Medicine, Columbia University, New York, New York 10032, United States.*

Kyungae Yang *- Department of Medicine, Columbia University, New York, New York 10032, United States.*

Tod Kippin *- Department of Psychological and Brain Sciences, University of California, Santa Barbara, Santa Barbara, California 93106, USA.*

Francesco Ricci *- Dipartimento di Scienze e Tecnologie Chimiche, University of Rome, Tor Vergata, Via della Ricerca Scientifica, 00133 Rome, Italy.*

Milan Stojanovic *- Department of Medicine, Columbia University, New York, New York 10032, United States; Department of Biomedical Engineering and Systems Biology, Columbia University, New York, New York 10032, USA.*

Kevin W. Plaxco *- Department of Chemistry and Biochemistry, University of California, Santa Barbara, Santa Barbara, California 93106, USA; Biomolecular Science and Engineering Program, University of California, Santa Barbara, Santa Barbara, California 93106; Biological Engineering Graduate Program, University of California Santa Barbara, Santa Barbara, CA 93106, USA; Department of Mechanical Engineering, University of California, Santa Barbara, Santa Barbara, California 93106, USA.*

AUTHOR CONTRIBUTIONS

The manuscript written through contributions of all authors. All authors have given approval to the final version of the manuscript. A.C, J.G., M.S., F.R., T.K. and K.P. designed the research; A.C, J.G., C.F., L.F., A.D., N.E., H.E., N.M. and K.Y. performed the research; A.C, J.G., T.D, F.R. and K.P.

analyzed and interpreted the data; A.C, J.G., F.R., T.K., M.S. and K.P. did manuscript writing and editing.

ACKNOWLEDGEMENTS

This work was supported by NIH grant EB022015. This project has received funding from the European Union's Horizon 2020 research and innovation program under the Marie Sklodowska-Curie grant agreement No 799332 (AC). A.C. was supported by Fondazione Umberto Veronesi postdoctoral Fellowship 2022. CF acknowledges support from an Otis Williams Postdoctoral Fellowship. The experimental protocol employed was approved by the institutional Animal Care and Use Committee (IACUC – protocol number 824) of the University of California Santa Barbara and adhered to the guidelines given by the NIH Guide for Care and Use of Laboratory Animals (IACUC, 2011).

SYNOPSIS TOC

Motivated by the pressing need for improved "therapeutic drug monitoring" we are developing minimally invasive biosensors for real-time monitoring of methotrexate levels in a live rat animal model.

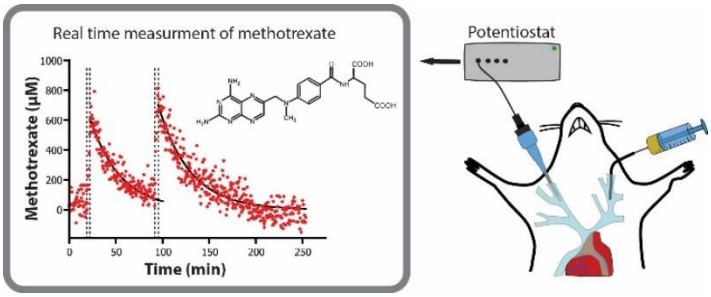

REFERENCES

(1) James, L.; Sullivan, J. E.; Roberts, D. The Proper Use of Acetaminophen. *Paediatr. Child Health* **2011**, *16* (9), 544–547.

(2) Bates, D. W.; Soldin, S. J.; Rainey, P. M.; Micelli, J. N. Strategies for Physician Education in Therapeutic Drug Monitoring. *Clin. Chem.* **1998**, *44* (2), 401–407.

(3) Widmer, N.; Bardin, C.; Chatelut, E.; Paci, A.; Beijnen, J.; Levêque, D.; Veal, G.; Astier, A. Review of Therapeutic Drug Monitoring of Anticancer Drugs Part Two – Targeted Therapies. *Eur. J. Cancer* **2014**, *50* (12), 2020–2036.

(4) Power, B. M.; Forbes, A. M.; van Heerden, P. V.; Ilett, K. F. Pharmacokinetics of Drugs Used in Critically Ill Adults. *Clin. Pharmacokinet.* **1998**, *34* (1), 25–56.

(5) Felici, A.; Verweij, J.; Sparreboom, A. Dosing Strategies for Anticancer Drugs: The Good, the Bad and Body-Surface Area. *Eur. J. Cancer* **2002**, *38* (13), 1677–1684.

(6) Undevia, S. D.; Gomez-Abuin, G.; Ratain, M. J. Pharmacokinetic Variability of Anticancer Agents. *Nat. Rev. Cancer* **2005**, *5* (6), 447–458.

(7) Franken, L. G.; Mathot, R. A. A.; Masman, A. D.; Baar, F. P. M.; Tibboel, D.; van Gelder, T.; Koch, B. C. P.; de Winter, B. C. M. Population Pharmacokinetics of Haloperidol in Terminally Ill Adult Patients. *Eur. J. Clin. Pharmacol.* **2017**, *73* (10), 1271–1277.

(8) Kang, J. S.; Lee, M. H. Overview of Therapeutic Drug Monitoring. *Korean J. Intern. Med.* **2009**, *24* (1), 1–10.

(9) Arroyo-Currás, N.; Somerson, J.; Vieira, P. A.; Ploense, K. L.; Kippin, T. E.; Plaxco, K. W. Real-Time Measurement of Small Molecules Directly in Awake, Ambulatory Animals. *Proc. Natl. Acad. Sci.* **2017**, *114* (4), 645 LP – 650.

(10) Arroyo-Currás, N.; Dauphin-Ducharme, P.; Ortega, G.; Ploense, K. L.; Kippin, T. E.; Plaxco, K. W. Subsecond-Resolved Molecular Measurements in the Living Body Using Chronoamperometrically Interrogated Aptamer-Based Sensors. *ACS Sensors* **2018**, *3* (2), 360–366.

(11) Dauphin-Ducharme, P.; Yang, K.; Arroyo-Currás, N.; Ploense, K. L.; Zhang, Y.; Gerson, J.; Kurnik, M.; Kippin, T. E.; Stojanovic, M. N.; Plaxco, K. W. Electrochemical Aptamer-Based Sensors for Improved Therapeutic Drug Monitoring and High-Precision, Feedback-Controlled Drug Delivery. *ACS Sensors* **2019**, *4* (10), 2832–2837.

(12) Idili, A.; Arroyo-Currás, N.; Ploense, K. L.; Csordas, A. T.; Kuwahara, M.; Kippin, T. E.; Plaxco, K. W. Seconds-Resolved Pharmacokinetic Measurements of the Chemotherapeutic Irinotecan in Situ in the Living Body. *Chem. Sci.* **2019**, *10* (35), 8164–8170.

(13) Heller, A. Integrated Medical Feedback Systems for Drug Delivery. *AIChE J.* **2005**, *51* (4), 1054–1066.

(14) Rosen, H.; Abribat, T. The Rise and Rise of Drug Delivery. *Nat. Rev. Drug Discov.* **2005**, *4* (5), 381–385.

(15) Xiao, Y.; Lubin, A. A.; Heeger, A. J.; Plaxco, K. W. Label-Free Electronic Detection of Thrombin in Blood Serum by Using an Aptamer-Based Sensor. *Angew. Chem. Int. Ed. Engl.* **2005**, *44* (34), 5456–5459.

(16) Xiao, Y.; Lai, R. Y.; Plaxco, K. W. Preparation of Electrode-Immobilized, Redox-Modified Oligonucleotides for Electrochemical DNA and Aptamer-Based Sensing. *Nat. Protoc.* **2007**, *2* (11), 2875–2880.

(17) Li, H.; Li, S.; Dai, J.; Li, C.; Zhu, M.; Li, H.; Lou, X.; Xia, F.; Plaxco, K. W. High Frequency, Calibration-Free Molecular Measurements in Situ in the Living Body. *Chem. Sci.* **2019**, *10* (47), 10843–10848.

(18) Idili, A.; Gerson, J.; Kippin, T.; Plaxco, K. W. Seconds-Resolved, In Situ Measurements of Plasma Phenylalanine Disposition Kinetics in Living Rats. *Anal. Chem.* **2021**, *93* (8), 4023–4032.

(19) Wilson, G. S.; Hu, Y. Enzyme-Based Biosensors for in Vivo Measurements. *Chem. Rev.* **2000**, *100* (7), 2693–2704.

(20) Bucher, E. S.; Wightman, R. M. Electrochemical Analysis of Neurotransmitters. *Annu. Rev. Anal. Chem. (Palo Alto. Calif).* **2015**, *8*, 239–261.

(21) Gowers, S. A. N.; Freeman, D. M. E.; Rawson, T. M.; Rogers, M. L.; Wilson, R. C.; Holmes, A. H.; Cass, A. E.; O'Hare, D. Development of a Minimally Invasive Microneedle-Based Sensor for Continuous Monitoring of β-Lactam Antibiotic Concentrations in Vivo. *ACS Sensors* **2019**, *4* (4), 1072–1080.

(22) Van Meter, A.; Williams, U.; Zavala, A.; Kee, J.; Rebello, E.; Tsai, J.; Ifeanyi, I.; Ruiz, J.; Lim, J.; Owusu-Agyemang, P. Beat to Beat: A Measured Look at the

History of Pulse Oximetry. *J. Anesth. Hist.* **2017**, *3* (1), 24–26.

(23) Vieira, P. A.; Shin, C. B.; Arroyo-Currás, N.; Ortega, G.; Li, W.; Keller, A. A.; Plaxco, K. W.; Kippin, T. E. Ultra-High-Precision, in-Vivo Pharmacokinetic Measurements Highlight the Need for and a Route Toward More Highly Personalized Medicine. *Front. Mol. Biosci.* **2019**, *6*, 69.

(24) Stoller, R. G.; Hande, K. R.; Jacobs, S. A.; Rosenberg, S. A.; Chabner, B. A. Use of Plasma Pharmacokinetics to Predict and Prevent Methotrexate Toxicity. *N. Engl. J. Med.* **1977**, *297* (12), 630–634.

(25) Guichard, N.; Guillarme, D.; Bonnabry, P.; Fleury-Souverain, S. Antineoplastic Drugs and Their Analysis: A State of the Art Review. *Analyst* **2017**, *142* (13), 2273–2321.

(26) Evans, W. E.; Pratt, C. B.; Taylor, R. H.; Barker, L. F.; Crom, W. R. Pharmacokinetic Monitoring of High-Dose Methotrexate. Early Recognition of High-Risk Patients. *Cancer Chemother. Pharmacol.* **1979**, *3* (3), 161–166.

(27) Le Guellec, C.; Blasco, H.; Benz, I.; Hulin, A. Therapeutic drug monitoring of methotrexate after its administration in high-dose protocols. *Therapie* **2010**, *65* (3), 163–169.

(28) Dombrowsky, E.; Jayaraman, B.; Narayan, M.; Barrett, J. S. Evaluating Performance of a Decision Support System to Improve Methotrexate Pharmacotherapy in Children and Young Adults with Cancer. *Ther. Drug Monit.* **2011**, *33* (1), 99–107.

(29) Pignon, T.; Lacarelle, B.; Duffaud, F.; Guillet, P.; Catalin, J.; Durand, A.; Favre, R. Dosage Adjustment of High-Dose Methotrexate Using Bayesian Estimation: A Comparative Study of Two Different Concentrations at the End of 8-h Infusions. *Ther. Drug Monit.* **1995**, *17* (5), 471–478.

(30) Masson, J.-F.; Pelletier, J. N. Will Nanobiosensors Change Therapeutic Drug Monitoring? The Case of Methotrexate. *Nanomedicine* **2015**, *10* (4), 521–524.

(31) Karami, F.; Ranjbar, S.; Ghasemi, Y.; Negahdaripour, M. Analytical Methodologies for Determination of Methotrexate and Its Metabolites in Pharmaceutical, Biological and Environmental Samples. *J. Pharm. Anal.* **2019**, *9* (6), 373–391.

(32) Hidi, I. J.; Mühlig, A.; Jahn, M.; Liebold, F.; Cialla, D.; Weber, K.; Popp, J. LOC-SERS: Towards Point-of-Care Diagnostic of Methotrexate. *Anal. Methods* **2014**, *6* (12), 3943–3947.

(33) Parachalil, D. R.; Commerford, D.; Bonnier, F.; Chourpa, I.; McIntyre, J.; Byrne, H. J. Raman Spectroscopy as a Potential Tool for Label Free Therapeutic Drug Monitoring in Human Serum: The Case of Busulfan and Methotrexate. *Analyst* **2019**, *144* (17), 5207–5214.

(34) He, J.; Wang, J.; Zhang, M.; Shi, G. Selection of a Structure-Switching Aptamer for the Specific Methotrexate Detection. *ACS Sensors* **2021**, *6* (6), 2436–2441.

(35) Zhao, S. S.; Bukar, N.; Toulouse, J. L.; Pelechacz, D.; Robitaille, R.; Pelletier, J. N.; Masson, J.-F. Miniature Multi-Channel SPR Instrument for Methotrexate Monitoring in Clinical Samples. *Biosens. Bioelectron.* **2015**, *64*, 664–670.

(36) Wu, Y.; Ranallo, S.; Del Grosso, E.; Chamorro-Garcia, A.; Ennis, H. L.; Milosavic, N.; Yang, K.; Kippin, T.; Ricci, F.; Stojanovic, M.; Plaxco, K. . Using Spectroscopy to Guide the Adaptation of Aptamers into Electrochemical Aptamer-Based Sensors. *Bioconjug. Chem.* **2022**, *Accepted.* (DOI: 10.1021/acs.bioconjchem.2c00275).

(37) Arroyo-Currás, N.; Scida, K.; Ploense, K. L.; Kippin, T. E.; Plaxco, K. W. High Surface Area Electrodes Generated via Electrochemical Roughening Improve the Signaling of Electrochemical Aptamer-Based Biosensors. *Anal. Chem.* **2017**, *89* (22), 12185–12191.

(38) Ferguson, B. S.; Hoggarth, D. A.; Maliniak, D.; Ploense, K.; White, R. J.; Woodward, N.; Hsieh, K.; Bonham, A. J.; Eisenstein, M.; Kippin, T. E.; Plaxco, K. W.; Soh, H. T. Real-Time, Aptamer-Based Tracking of Circulating Therapeutic Agents in Living Animals. *Sci. Transl. Med.* **2013**, *5* (213), 213ra165.

(39) Downs, A. M.; Gerson, J.; Leung, K. K.; Honeywell, K. M.; Kippin, T.; Plaxco, K. W. Improved Calibration of Electrochemical Aptamer-Based Sensors. *Sci. Rep.* **2022**, *12* (1), 5535.

(40) Dauphin-Ducharme, P.; Ploense, K. L.; Arroyo-Currás, N.; Kippin, T. E.; Plaxco, K. W. Electrochemical Aptamer-Based Sensors: A Platform Approach to High-Frequency Molecular Monitoring In Situ in the Living Body BT - Biomedical Engineering Technologies: Volume 1; Ossandon, M. R., Baker, H., Rasooly, A., Eds.; Springer US: New York, NY, 2022; pp 479–492.

(41) Arroyo-Currás, N.; Ortega, G.; Copp, D. A.; Ploense, K. L.; Plaxco, Z. A.; Kippin, T. E.; Hespanha, J. P.; Plaxco, K. W. High-Precision Control of Plasma Drug Levels Using Feedback-Controlled Dosing. *ACS Pharmacol. Transl. Sci.* **2018**, *1* (2), 110–118.

(42) Bore, P.; Bruno, R.; Lena, N.; Favre, R.; Cano, J. P. Methotrexate and 7-Hydroxy-Methotrexate Pharmacokinetics Following Intravenous Bolus Administration and High-Dose Infusion of Methotrexate. *Eur. J. Cancer Clin. Oncol.* **1987**, *23* (9), 1385–1390.

(43) Barreto, J. N.; Reid, J. M.; Thompson, C. A.; Mara, K. C.; Rule, A. D.; Kashani, K. B.; Leung, N.; Larson, T. R.; McGovern, R. M.; Witzig, T. E.; Barreto, E. F. Prospective Evaluation of High-Dose Methotrexate Pharmacokinetics in Adult Patients with Lymphoma Using Novel Determinants of Kidney Function. *Clin. Transl. Sci.* **2022**, *15* (1), 105–117.

(44) Bremnes, R. M.; Slørdal, L.; Wist, E.; Aarbakke, J. Dose-Dependent Pharmacokinetics of Methotrexate and 7-Hydroxymethotrexate in the Rat in Vivo. *Cancer Res.* **1989**, *49* (22), 6359–6364.

(45) Pignon, T.; Lacarelle, B.; Duffaud, F.; Guillet, P.; Catalin, J.; Durand, A.; Monjanel, S.; Favre, R. Pharmacokinetics of High-Dose Methotrexate in Adult Osteogenic Sarcoma. *Cancer Chemother. Pharmacol.* **1994**, *33* (5), 420–424.

(46) Fuskevåg, O.-M.; Kristiansen, C.; Lindal, S.; Aarbakke, J. Maximum Tolerated Doses of Methotrexate and 7-Hydroxy-Methotrexate in a Model of Acute Toxicity in Rats. *Cancer Chemother. Pharmacol.* **2000**, *46* (1), 69–73.

(47) Bischoff, K. B.; Dedrick, R. L.; Zaharko, D. S.; Longstreth, J. A. Methotrexate Pharmacokinetics. *J. Pharm. Sci.* **1971**, *60* (8), 1128–1133.
(48) Scheufler, E.; Zetler, G.; Iven, H. Pharmacokinetics and Organ Distribution of Methotrexate in the Rat. *Pharmacology* **1981**, *23* (2), 75–81.
(49) Ivarsson, L.; Appelgren, L.; Rudenstam, C.-M. Plasma Volume after Dextran Infusion in Rats Sensitive and Non-Sensitive to Dextran. *Eur. Surg. Res.* **1975**, *7* (6), 315–325.
(50) Taylor, I. M.; Du, Z.; Bigelow, E. T.; Eles, J. R.; Horner, A. R.; Catt, K. A.; Weber, S. G.; Jamieson, B. G.; Cui, X. T. Aptamer-Functionalized Neural Recording Electrodes for the Direct Measurement of Cocaine in Vivo. *J. Mater. Chem. B* **2017**, *5* (13), 2445–2458.
(51) Ekstrøm, O.; Andersen, A.; Warren, D. J.; Giercksky, K. E.; Slørdal, L. Evaluation of Methotrexate Tissue Exposure by in Situ Microdialysis in a Rat Model. *Cancer Chemother. Pharmacol.* **1994**, *34* (4), 297–301.
(52) Liu, D.-Y.; Lon, H.-K.; Wang, Y.-L.; DuBois, D. C.; Almon, R. R.; Jusko, W. J. Pharmacokinetics, Pharmacodynamics and Toxicities of Methotrexate in Healthy and Collagen-Induced Arthritic Rats. *Biopharm. Drug Dispos.* **2013**, *34* (4), 203–214.
(53) Abrey, L. E.; DeAngelis, L. M.; Yahalom, J. Long-Term Survival in Primary CNS Lymphoma. *J. Clin. Oncol. Off. J. Am. Soc. Clin. Oncol.* **1998**, *16* (3), 859–863.
(54) Howard, S. C.; McCormick, J.; Pui, C.-H.; Buddington, R. K.; Harvey, R. D. Preventing and Managing Toxicities of High-Dose Methotrexate. *Oncologist* **2016**, *21* (12), 1471–1482.
(55) Widemann, B. C.; Balis, F. M.; Kim, A.; Boron, M.; Jayaprakash, N.; Shalabi, A.; O'Brien, M.; Eby, M.; Cole, D. E.; Murphy, R. F.; Fox, E.; Ivy, P.; Adamson, P. C. Glucarpidase, Leucovorin, and Thymidine for High-Dose Methotrexate-Induced Renal Dysfunction: Clinical and Pharmacologic Factors Affecting Outcome. *J. Clin. Oncol.* **2010**, *28* (25), 3979–3986.
(56) Redlarski, G.; Palkowski, A.; Krawczuk, M. Body Surface Area Formulae: An Alarming Ambiguity. *Sci. Rep.* **2016**, *6* (1), 27966.
(57) Pai, M. P.; Debacker, K. C.; Derstine, B.; Sullivan, J.; Su, G. L.; Wang, S. C. Comparison of Body Size, Morphomics, and Kidney Function as Covariates of High-Dose Methotrexate Clearance in Obese Adults with Primary Central Nervous System Lymphoma. *Pharmacotherapy* **2020**, *40* (4), 308–319.
(58) Seideman, P.; Beck, O.; Eksborg, S.; Wennberg, M. The Pharmacokinetics of Methotrexate and Its 7-Hydroxy Metabolite in Patients with Rheumatoid Arthritis. *Br. J. Clin. Pharmacol.* **1993**, *35* (4), 409–412.
(59) Chládek, J.; Grim, J.; Martínková, J.; Simková, M.; Vanìèková, J.; Koudelková, V.; Noièková, M. Pharmacokinetics and Pharmacodynamics of Low-Dose Methotrexate in the Treatment of Psoriasis. *Br. J. Clin. Pharmacol.* **2002**, *54* (2), 147–156.
(60) Ramsey, L. B.; Balis, F. M.; O'Brien, M. M.; Schmiegelow, K.; Pauley, J. L.; Bleyer, A.; Widemann, B. C.; Askenazi, D.; Bergeron, S.; Shirali, A.; Schwartz, S.; Vinks, A. A.; Heldrup, J. Consensus Guideline for Use of Glucarpidase in Patients with High-Dose Methotrexate Induced Acute Kidney Injury and Delayed Methotrexate Clearance. *Oncologist* **2018**, *23* (1), 52–61.
(61) Mc Laughlin, A. M.; Schmulenson, E.; Teplytska, O.; Zimmermann, S.; Opitz, P.; Groenland, S. L.; Huitema, A. D. R.; Steeghs, N.; Müller, L.; Fuxius, S.; Illerhaus, G.; Joerger, M.; Mayer, F.; Fuhr, U.; Holdenrieder, S.; Hempel, G.; Scherf-Clavel, O.; Jaehde, U.; Kloft, C.; Consortium, F. T. O.-T. S. Developing a Nationwide Infrastructure for Therapeutic Drug Monitoring of Targeted Oral Anticancer Drugs: The ON-TARGET Study Protocol. *Cancers (Basel).* **2021**, *13* (24), 6281.
(62) Mage, P. L.; Ferguson, B. S.; Maliniak, D.; Ploense, K. L.; Kippin, T. E.; Soh, H. T. Closed-Loop Control of Circulating Drug Levels in Live Animals. *Nat. Biomed. Eng.* **2017**, *1* (5), 70.